

Constitutive expression of murine c-FLIP_R causes autoimmunity in aged mice

F Ewald^{1,2}, M Annemann^{1,2}, MC Pils³, C Plaza-Sirvent^{1,2}, F Neff⁴, C Erck⁵, D Reinhold¹ and I Schmitz^{*,1,2}

Death receptor-mediated apoptosis is a key mechanism for the control of immune responses and dysregulation of this pathway may lead to autoimmunity. Cellular FLICE-inhibitory proteins (c-FLIPs) are known as inhibitors of death receptor-mediated apoptosis. The only short murine c-FLIP splice variant is c-FLIP_{Raji} (c-FLIP_R). To investigate the functional role of c-FLIP_R in the immune system, we used the vavFLIP_R mouse model constitutively expressing murine c-FLIP_R in all hematopoietic compartments. Lymphocytes from these mice are protected against CD95-mediated apoptosis and activation-induced cell death. Young vavFLIP_R mice display normal lymphocyte compartments, but the lymphocyte populations alter with age. We identified reduced levels of T cells and slightly higher levels of B cells in 1-year-old vavFLIP_R mice compared with wild-type (WT) littermates. Moreover, both B and T cells from aged vavFLIP_R animals show activated phenotypes. Sera from 1-year-old WT and transgenic animals were analysed for anti-nuclear antibodies. Notably, elevated titres of these autoantibodies were detected in vavFLIP_R sera. Furthermore, tissue damage in kidneys and lungs from aged vavFLIP_R animals was observed, indicating that vavFLIP_R mice develop a systemic lupus erythematosus-like phenotype with age. Taken together, these data suggest that c-FLIP_R is an important modulator of apoptosis and enforced expression leads to autoimmunity.

Cell Death and Disease (2014) 5, e1168; doi:10.1038/cddis.2014.138; published online 10 April 2014

Subject Category: Immunity

It is crucial that excessive lymphocytes are deleted by apoptosis after efficient antigen clearance to maintain cell homeostasis.¹ Moreover, insufficient apoptosis of auto-reactive immune cells may result in autoimmune diseases.¹ The extrinsic apoptosis pathway is triggered by ligand binding of death receptors, such as CD95 (Fas/APO-1), and regulates the removal of unwanted lymphocytes.² Elimination of T cells is achieved by activation-induced cell death (AICD), which is triggered upon restimulation of T cells without co-stimulation.² Notably, the CD95 death receptor pathway was shown to be important for AICD.^{3–6} Furthermore, dysregulation of the CD95 signalling pathway was reported to result in severely altered lymphoproliferation (*Lpr*) and autoimmunity in both *lpr* and *generalised lymphoproliferative disorder (gld)* mice, which have mutated CD95 receptor or ligand, respectively, as well as in patients suffering from the homologous human disease autoimmune lymphoproliferative syndrome.^{7,8} CD95 is the best-characterised death receptor and it is activated by binding of its cognate ligand CD95L.⁹ Ligand-binding results in

receptor oligomerisation and formation of the death-inducing signalling complex (DISC) through recruitment of the proteins Fas-associated death domain-containing protein (FADD), procaspase-8, -10 and cellular FLICE-inhibitory protein (c-FLIP).¹⁰ Autoproteolytic processing of procaspase-8 at the DISC generates active caspase-8,^{11,12} which cleaves and activates caspase-3 and -7. The effector caspases process further substrates, eventually leading to apoptosis.^{13,14} The c-FLIPs inhibit apoptosis by competing with procaspase-8 for binding sites at the DISC and additionally interfere with caspase-8 processing.^{15–17} So far, three c-FLIP isoforms expressed on the protein level have been reported: c-FLIP_{Long} (c-FLIP_L), c-FLIP_{Short} (c-FLIP_S) and c-FLIP_{Raji} (c-FLIP_R).^{15,17,18} The long isoform resembles caspase-8, but lacks catalytic function because of substitution of amino-acid residues critical for enzymatic activity.^{18,19} The two short isoforms are distinguished by a functional nucleotide polymorphism and mainly consist of the death effector domains with unique C-terminal tails.²⁰ The structure of the murine

¹Institute of Molecular and Clinical Immunology, Otto-von-Guericke-University Magdeburg, Leipziger Str. 44, Magdeburg, Germany; ²Research Group of Systems-Oriented Immunology and Inflammation Research, Department of Immune Control, Helmholtz Centre for Infection Research, Inhoffenstr. 7, Braunschweig, Germany;

³Mouse Pathology, Animal Experimental Unit, Helmholtz Centre for Infection Research, Inhoffenstr. 7, Braunschweig, Germany; ⁴Institute of Pathology, Helmholtz Centre Munich, Ingolstaedter Landstr. 1, Neuherberg, Germany and ⁵Cellular Proteome Research, Department of Structure and Function of Proteins, Helmholtz Centre for Infection Research, Inhoffenstr. 7, Braunschweig, Germany

*Corresponding author: I Schmitz, Institute of Molecular and Clinical Immunology, Otto-von-Guericke-University Magdeburg, Leipziger Str. 44, Magdeburg, Germany or Research Group of Systems-Oriented Immunology and Inflammation Research, Department of Immune Control, Helmholtz Centre for Infection Research, Inhoffenstr. 7, D-38124, Braunschweig, Germany. Tel: +49 531 61813500; Fax: +49 531 61813599; E-mail: ingo.schmitz@helmholtz-hzi.de

Keywords: c-FLIP; apoptosis; CD95; autoimmunity

Abbreviations: AICD, activation-induced cell death; ANA, anti-nuclear antibody; BALT, bronchial-associated lymphoid tissue; *Cflar*, caspase-8 and FADD-like apoptosis regulator; c-FLIP_L, cellular FLICE-inhibitory protein, long isoform; c-FLIP_S, cellular FLICE-inhibitory protein, short isoform; c-FLIP_R, cellular FLICE-inhibitory protein, Raji isoform; CNS, central nervous system; DC, dendritic cell; DISC, death-inducing signalling complex; DN, double negative; EAE, experimental autoimmune encephalomyelitis; FADD, Fas-associated death domain-containing protein; *Gld*, generalised lymphoproliferative disorder; IFN- γ , interferon- γ ; *Lpr*, lymphoproliferation; MOG, myelin oligodendrocyte glycoprotein; MS, multiple sclerosis; SLE, systemic lupus erythematosus; WT, wild type

Received 05.9.13; revised 27.2.14; accepted 28.2.14; Edited by M Leverkus

Cflar (*caspase-8* and *FADD-like apoptosis regulator*) gene differs from the human gene locus, in that only c-FLIP_L and c-FLIP_R can be expressed.²¹ Although the short c-FLIP isoforms have been described as anti-apoptotic, c-FLIP_L was reported to act both pro- and anti-apoptotic depending on expression level and strength of receptor stimulation.^{22–24} Transgenic overexpression of c-FLIP_L in mice resulted in autoimmunity, although only in the Balb/c background.²⁵ In contrast, mice overexpressing human c-FLIP_S did not develop autoimmune disease.^{26,27} Not much is known about the physiological function of c-FLIP_R. To investigate the functional role of c-FLIP_R in the immune system, we used a mouse model, called vavFLIP_R, with constitutive expression of murine c-FLIP_R in all hematopoietic compartments. We previously reported that these transgenic mice have a better clearance of the Gram-positive bacteria *Listeria monocytogenes* compared with infected wild-type (WT) mice.²⁸ Here we show that aged mice constitutively expressing murine c-FLIP_R have altered lymphocyte populations with higher levels of activated B and T cells compared with WT littermates. Moreover, vavFLIP_R animals spontaneously develop autoimmunity with age, showing features of systemic lupus erythematosus (SLE).

Results

vavFLIP_R mice do not recapitulate the *lpr/gld* phenotype.

Insufficient cell death can lead to autoimmunity as a result of altered immune cell populations. *Lpr* and *gld* mice, with mutations in the CD95 receptor and ligand, respectively, develop *Lpr* and autoimmunity.^{7,29} Moreover, these mice accumulate unusual CD4⁺ CD8[−] double negative (DN)

B220⁺ αβ T cells.^{7,30} c-FLIP_R inhibits apoptosis by competing with caspase-8 for binding sites at the DISC.^{17,21} The mouse model vavFLIP_R, in which murine c-FLIP_R is under control of the *vav*-promoter to ensure expression in all hematopoietic compartments,²⁸ was used to study the functional role of murine c-FLIP_R in the immune system. As thymocytes as well as B and T cells from vavFLIP_R mice were protected against CD95-induced apoptosis,²⁸ we investigated if the impaired lymphocyte apoptosis in vavFLIP_R mice would lead to elevated numbers of lymphocytes and altered lymphocyte populations with age. No *Lpr* was identified in 12–14 months old vavFLIP_R animals. In fact, the number of cells in the peripheral lymph nodes (pLNs) from vavFLIP_R mice was reduced compared with WT littermates (Figure 1a). Furthermore, pLN cells of WT and vavFLIP_R mice were analysed for DN B220⁺ T cells compared with 3 months old MRL/*lpr* mice as controls. The characteristic DN B220⁺ population was identified in MRL/*lpr* mice, but was not observed in either WT or vavFLIP_R animals (Figure 1b). The lack of DN B220⁺ T cells in vavFLIP_R mice is similar to the phenotype of c-FLIP_L transgenic mice³¹ and mice with transgenic expression of human c-FLIP_S.²⁷ Thus, vavFLIP_R mice do not develop an *lpr/gld*-like phenotype.

Altered lymphocyte populations in aged vavFLIP_R mice.

Young vavFLIP_R mice displayed normal lymphocyte populations.²⁸ We analysed aged WT and vavFLIP_R mice to investigate if the constitutive expression of c-FLIP_R alters lymphocyte populations over time. Dendritic cells (DCs), macrophages and granulocytes have been reported to be regulated through death receptors and c-FLIP proteins.^{32,33} We therefore analysed the frequencies of CD11c⁺ DCs,

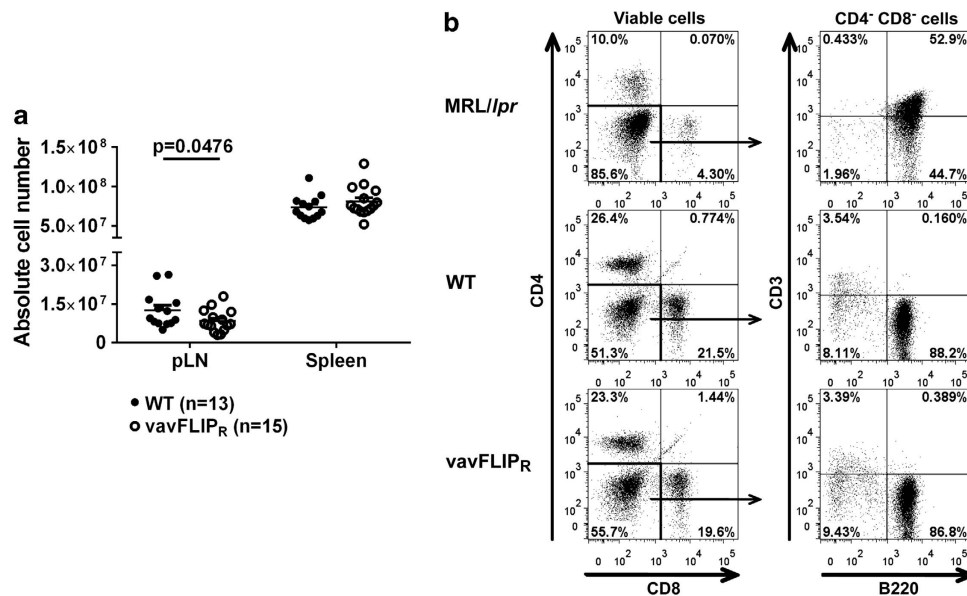


Figure 1 One-year-old vavFLIP_R mice display normal cellularity in lymphoid organs and do not accumulate DN B220⁺ cells. (a) Absolute cell numbers in pLNs and spleens of WT (*n* = 13) and vavFLIP_R (*n* = 15) mice at 12–14 months of age. Symbols represent individual mice, horizontal lines display the mean ± S.E.M. pooled from five independent experiments. Statistical analysis was performed with two-tailed nonparametric Mann–Whitney *U*-test. (b) Analysis of DN B220⁺ cells in pLNs from 1-year-old WT and vavFLIP_R animals. Representative dot plots are shown for MRL/*lpr* (*n* = 2), WT (*n* = 6) and vavFLIP_R (*n* = 7) mice. Three months old MRL/*lpr* mice develop the characteristic DN B220⁺ cells (upper panel). This subset could not be identified in either WT (mid panel) or vavFLIP_R mice (lower panel)

CD49b⁺ natural killer (NK) cells, F4/80⁺ macrophages and Gr1⁺ granulocytes in 1-year-old mice. The populations of CD11c⁺, CD49b⁺, F4/80⁺ and Gr1⁺ cells from WT and vavFLIP_R were comparable (Supplementary Table 1). Flow cytometry analyses of lymphocyte sub-populations in spleen and pLNs from 12 to 14 months old mice revealed reduced frequencies of vavFLIP_R CD3⁺ T cells compared with WT CD3⁺ T cells (Figures 2a and b), consistent with reduced absolute CD3⁺ T-cell number in pLNs from vavFLIP_R animals (Figure 2c). Furthermore, an increased percentage of vavFLIP_R CD19⁺ B cells in pLNs compared with WT was observed (Figures 2a and d). Frequencies and absolute numbers of CD19⁺ B cells were not significantly altered in the spleen (Figure 2e). Neither did we detect alterations in germinal centre formation in aged transgenic mice (data not shown). The CD4⁺/CD8⁺ cell profiles within the CD3⁺ T-cell compartment were comparable between WT and vavFLIP_R mice (Supplementary Figure 1). Nevertheless, lower frequencies of splenic CD8⁺ T cells were observed as well as reduced absolute cell numbers of CD8⁺ cells in pLNs (Supplementary Figure 1b). As we previously reported that thymocyte development in vavFLIP_R mice is normal,²⁸ we suggest that c-FLIP_R

expression regulates homeostasis of peripheral CD8⁺ T cells. Taken together, the B- and T-cell populations are altered in aged vavFLIP_R mice, whereas other haematopoietic cells are unaffected.

Activated phenotypes of T and B cells from vavFLIP_R mice. The activation status of T cells in young vavFLIP_R mice was comparable to WT littermates.²⁸ As AICD is impaired in T cells from vavFLIP_R mice,²⁸ we investigated if the activation status changed with age. We observed higher percentages of vavFLIP_R CD4⁺ cells expressing the activation marker CD25 in comparison with WT CD4⁺ cells (Figures 3a and b), with absolute cell numbers being similar between 12 and 14 months old WT and vavFLIP_R mice (Figure 3c). As CD25 is not only a marker for activated T cells, but is also highly expressed on regulatory T (T_{reg}) cells,³⁴ we analysed the expression of the master transcription factor of T_{reg} cells, Foxp3.³⁵ Indeed, most of the CD25⁺ CD4⁺ T cells co-expressed Foxp3 indicating that 1-year-old vavFLIP_R mice have higher levels of T_{reg} cells in both pLNs (Figure 3d) and spleen (data not shown) compared with WT littermates. Interestingly, we also observed an increase in CD25⁺ T cells that were negative for Foxp3 suggesting that

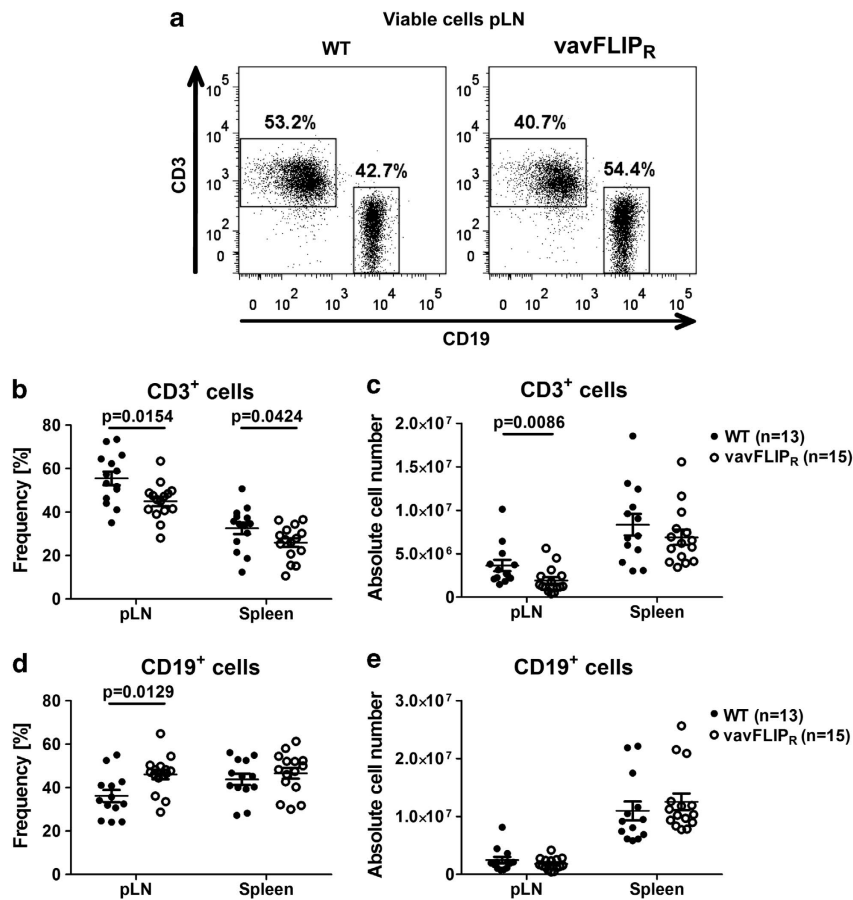


Figure 2 Altered lymphocyte populations in 12–14 months old vavFLIP_R mice. (a) Representative dot plots of CD3- and CD19-stained WT and vavFLIP_R pLN cells. Frequency and absolute cell number of CD3⁺ cells (b and c) and CD19⁺ cells (d and e) in freshly isolated pLNs and spleens from WT (*n* = 13) and vavFLIP_R (*n* = 15) littermates. Individual mice are represented as separate symbols. Horizontal lines show the mean pooled from five independent experiments; error bars display the S.E.M. Statistical analyses were performed with two-tailed nonparametric Mann–Whitney *U*-tests

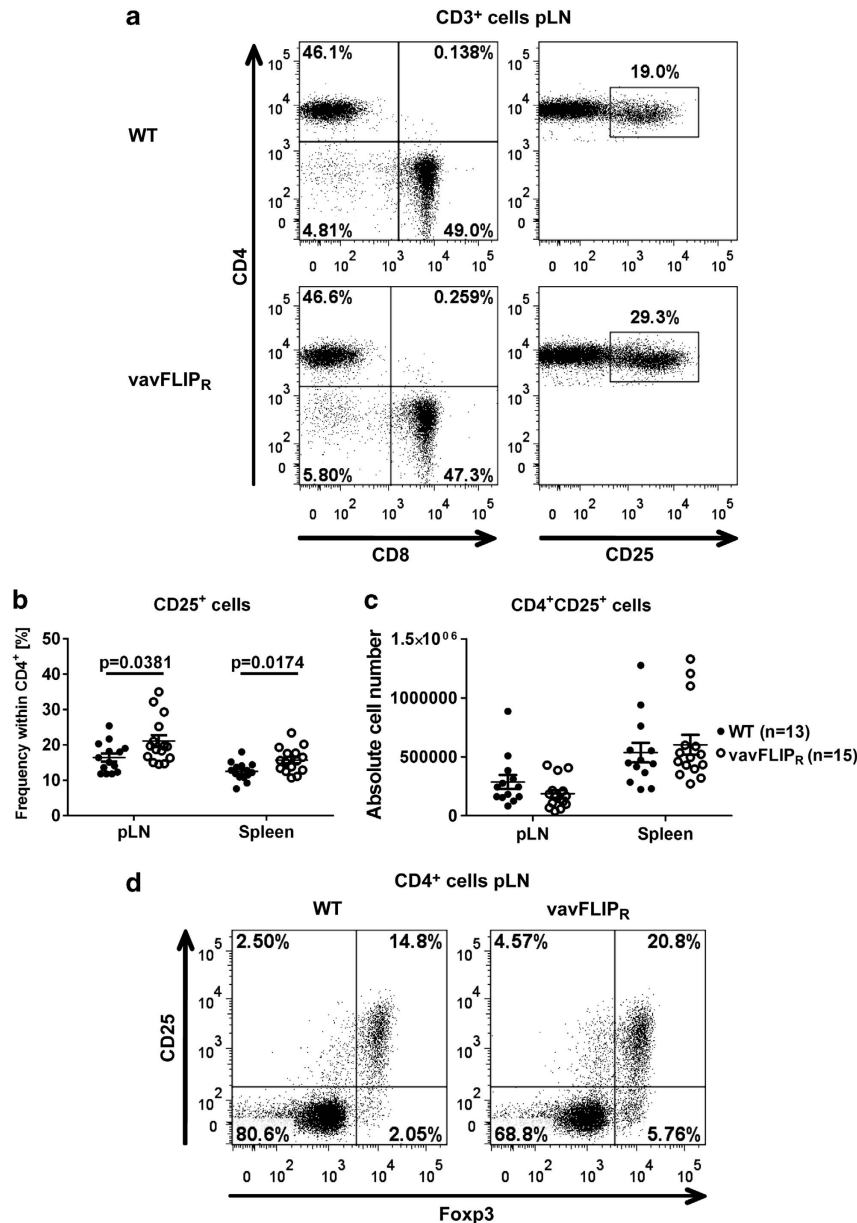


Figure 3 Increased levels of CD25⁺ T cells and T_{reg} cells in 1-year-old vavFLIP_R animals. (a) Representative dot plots of WT (upper panel) and vavFLIP_R (lower panel) CD3⁺ cells in pLNs. Frequency (b) and absolute cell number (c) of CD4⁺CD25⁺ cells in WT (*n* = 13) and vavFLIP_R (*n* = 15) pLN and spleens. Symbols represent individual mice. Horizontal lines display the mean ± S.E.M. Statistical analyses were performed with two-tailed nonparametric Mann–Whitney *U*-tests. (d) Dot plots showing CD25⁺ and Foxp3⁺ T cells within the CD4⁺ compartment representative for three WT (left) and four vavFLIP_R (right) mice

conventional T cells may indeed be more activated (Figure 3d). Therefore, the memory/naive T-cell profile was analysed in 12–14 months old WT and vavFLIP_R animals. Strikingly, elevated frequencies of CD44⁺ antigen-experienced cells within the CD3⁺ compartment were identified in both pLNs and spleen from vavFLIP_R mice (Figures 4a and b). We also observed reduced numbers of CD3⁺CD62L⁺ naive T cells in vavFLIP_R animals (Supplementary Figure 2a). Notably, both within the CD4⁺ helper T-cell population and the CD8⁺ cytotoxic T-cell population from vavFLIP_R pLNs and spleens, higher levels of antigen-experienced (CD44⁺) cells and lower levels of

naive (CD62L⁺) cells were identified compared with WT (Figures 4c and d). The absolute cell numbers of CD62L⁺ cells were reduced for both CD4⁺ and CD8⁺ T-cell populations (Supplementary Figures 2b and c). These data indicate that T cells from vavFLIP_R mice are highly activated in comparison with WT T cells.

Similar to T cells, B cells from vavFLIP_R mice are protected against apoptosis.²⁸ The activation status of B cells was examined by flow cytometry. CD40, CD80 and CD95 had similar expression levels in vavFLIP_R and WT animals (data not shown), whereas analysis of the activation markers CD69, CD86 and major histocompatibility complex class II molecule

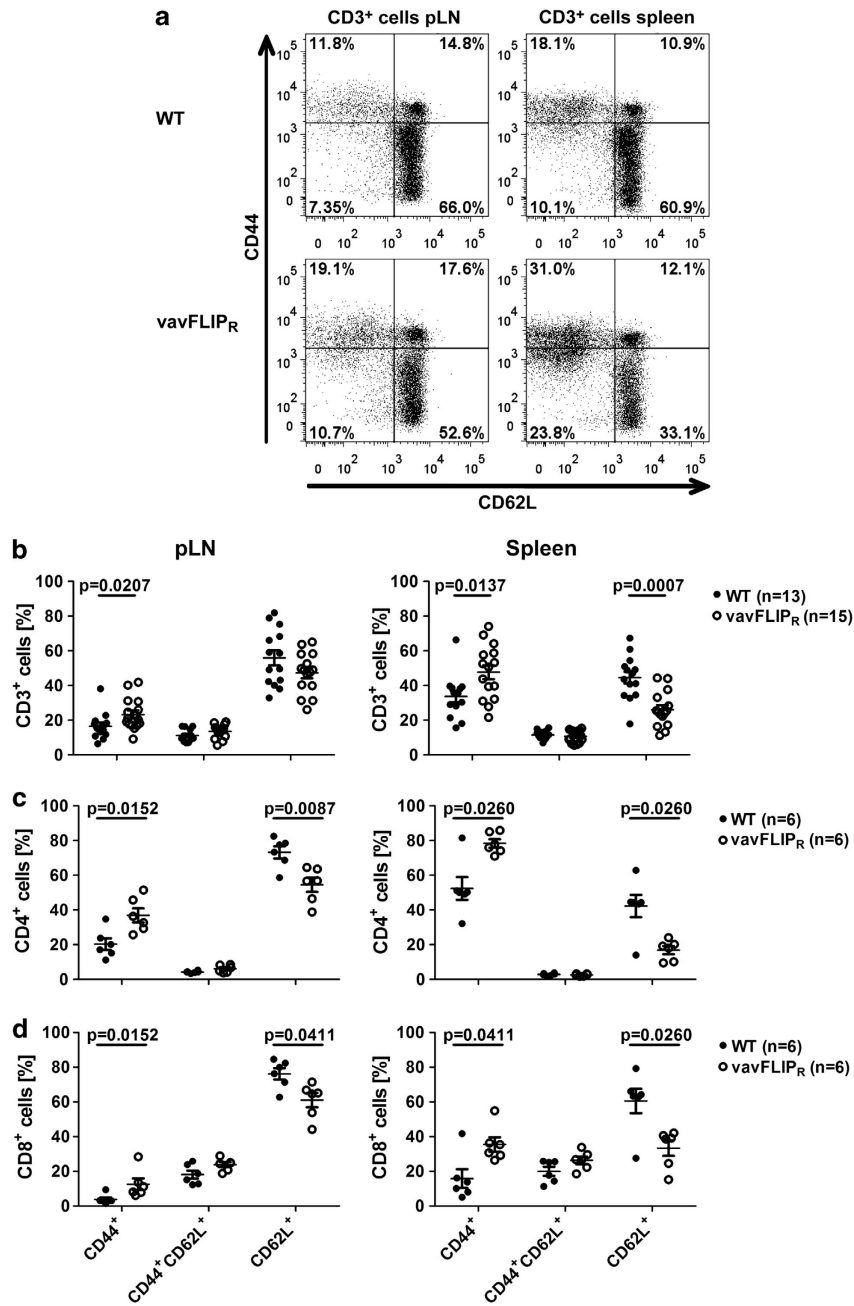


Figure 4 T cells from vavFLIP_R mice at 12–14 months of age are highly activated. (a) Representative dot plots of pLN cells (left panel) and splenocytes (right panel) from WT (upper panel) and vavFLIP_R animals (lower panel). Frequencies of CD44⁺, CD44⁺ CD62L⁺ and CD62L⁺ cells within CD3⁺ cells (b), CD4⁺ cells (c) and CD8⁺ cells (d) from pLN and spleen. (b–d) Symbols represent individual WT (b: n = 13, c and d: n = 6) and vavFLIP_R (b: n = 15, c and d: n = 6) mice. Horizontal lines represent (b) the mean pooled from five independent experiments or (c and d) the mean of one experiment representative for two independent experiments; error bars display S.E.M. Statistical analyses were performed with two-tailed nonparametric Mann–Whitney *U*-tests

I-A/I-E revealed an increased expression of these markers in vavFLIP_R B cells compared with WT B cells (Figure 5). This indicates that B cells from 12 to 14 months old vavFLIP_R mice are more activated in comparison with B cells from WT animals at 1 year of age. The activated phenotypes of B and T cells identified in 1-year-old vavFLIP_R mice are consistent with a previous study, which reported that B and T cells from c-FLIP_L transgenic mice on a Balb/c background were highly activated.²⁵

Disease progression in MOG-EAE is comparable between WT and vavFLIP_R mice. As constitutive expression of c-FLIP_R alters lymphocyte populations and activation status with age, we investigated if this has functional relevance in T-cell-mediated autoimmune disease. Experimental autoimmune encephalomyelitis (EAE) is a widely accepted animal model for studying the human demyelinating inflammatory disorder multiple sclerosis (MS).³⁶ T_H1 and T_H17 effector T cells have been shown to

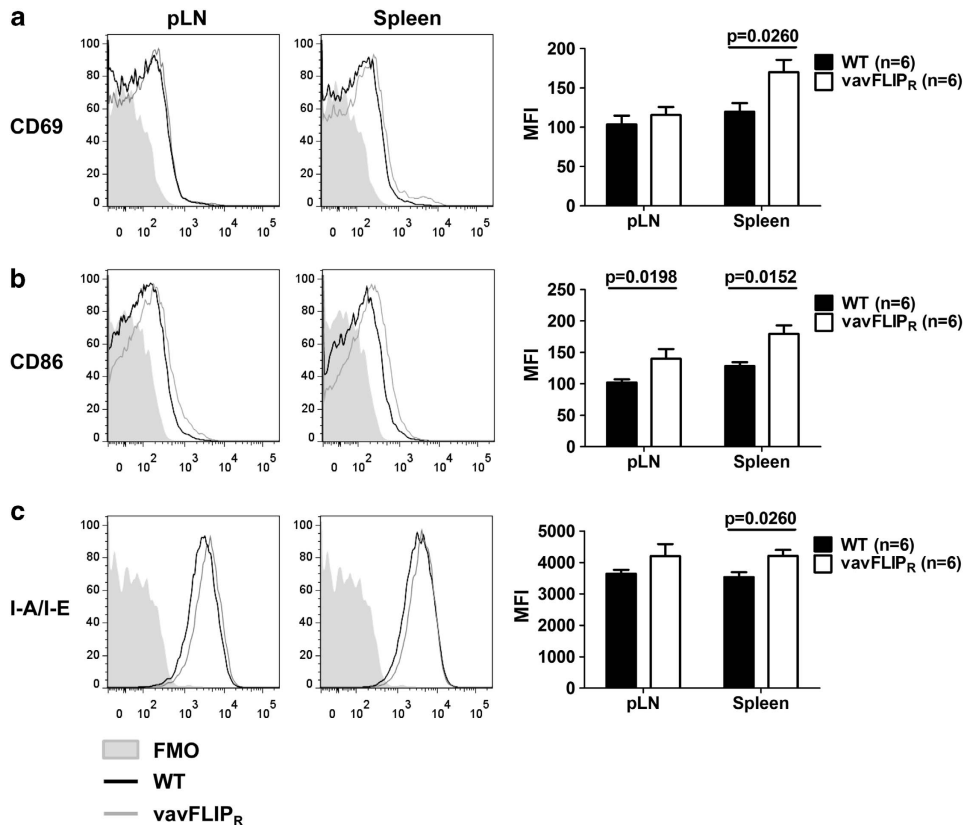


Figure 5 vavFLIP_R B cells from 12 to 14 months old mice show an activated phenotype. (a–c) pLN cells and splenocytes from WT and vavFLIP_R mice ($n=6$) were isolated and analysed by flow cytometry. The activation status of CD19⁺ B cells was assayed by the markers CD69 (a), CD86 (b) and I-A/I-E (c). Representative histograms with fluorescent minus one (FMO) as control (left panel) and diagrams displaying the mean fluorescent intensity (MFI; right panel) \pm S.E.M. are shown. Statistical analyses were performed with two-tailed nonparametric Mann–Whitney *U*-tests

contribute to the pathology in EAE³⁷ and c-FLIP_L transgenic mice were reported to be resistant to myelin oligodendrocyte glycoprotein (MOG)-EAE because of enhanced T_H2, and thus diminished T_H1, effector responses.³⁸ To assess if c-FLIP_R influences the differentiation of T_H0, T_H1, T_H2 or T_H17 cells, we cultured naive WT and vavFLIP_R T cells under T_H1, T_H2 or T_H17 polarising conditions *in vitro*. The frequencies of interferon- γ (IFN- γ)-producing T_H1 cells were comparable between WT and vavFLIP_R differentiated T cells (Figures 6a and b). Interestingly, frequencies in IL-17A-producing T_H17 cells and IL-4 mRNA induction in T_H2 cells were lower in vavFLIP_R T cells cultured under the respective polarising conditions (Figures 6a, b and c).

WT and vavFLIP_R mice were immunised with the MOG₃₅₋₅₅ peptide in complete Freund's adjuvant in conjunction with pertussis toxin to investigate if constitutive murine c-FLIP_R expression in T cells, macrophages and DCs influences EAE disease. However, both WT and vavFLIP_R animals developed disease with neurological defects resulting in paralysis of the tail and muscle weakness with comparable severity of disease. Only a slightly slower disease progression was observed in vavFLIP_R mice (Figure 6d). To investigate whether T-cell effector responses were affected by the transgenic expression of c-FLIP_R *in vivo*, we analysed cytokine production in MOG-peptide restimulated T cells from MOG-immunised mice. We observed slightly reduced

frequencies of IFN- γ ⁺ and IL-17A⁺ cells from vavFLIP_R pLNs in comparison with WT 11 days after immunisation (Figure 6e). This effect was levelled out at higher MOG peptide concentrations on day 14 (Figure 6e). The frequencies of IL-4-producing T cells in pLNs from vavFLIP_R and WT mice were comparable (Figure 6e). Similar results were obtained when T cells were restimulated in a polyclonal manner, that is, with anti-CD3 and anti-CD28 (Supplementary Figure 3). In summary, our data indicate a minor defect in vavFLIP_R effector T-cell responses that results in a slight delay in EAE disease progression in vavFLIP_R mice.

Elevated ANA-titres and tissue damage of kidneys and lungs in aged vavFLIP_R mice. B-cell-mediated autoimmunity is characterised by autoantibodies targeting the body's own tissues. As vavFLIP_R mice had slightly higher B-cell levels with activated phenotype, we analysed sera from 1-year-old WT and vavFLIP_R mice for anti-nuclear antibodies (ANAs) using an indirect immunofluorescence assay with HEp-2 cells as source of nuclear antigens. Negative fluorescent pattern was most often observed when sera from WT mice were incubated on HEp-2 cells (Figure 7a), whereas homogenous fluorescent pattern was detected for the majority of sera from vavFLIP_R mice even at high serum dilution (Figure 7b). Hence, significantly more

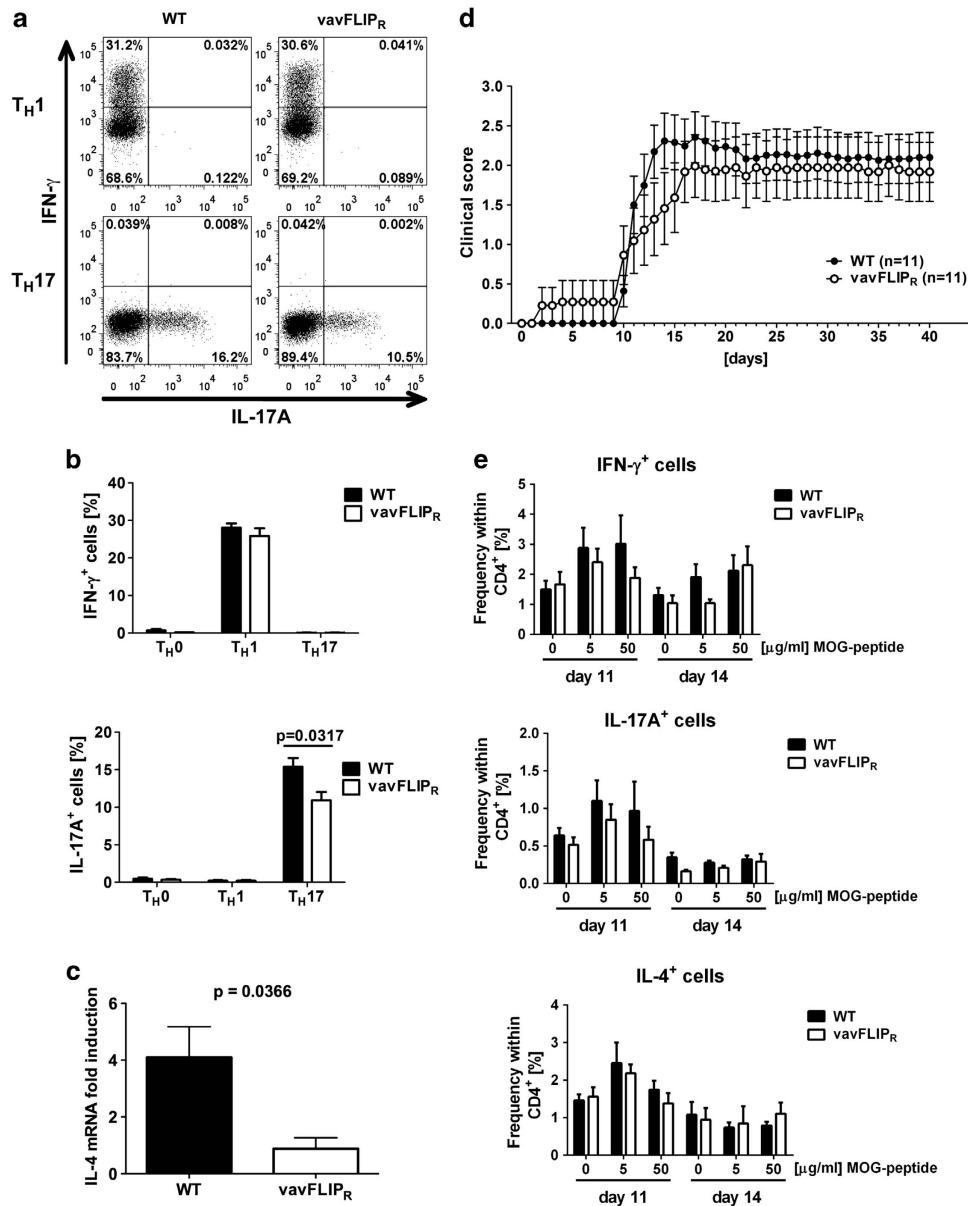


Figure 6 Comparable disease progression in MOG₃₅₋₅₅-peptide-induced EAE in WT and vavFLIP_R mice. (a–c) Naive T cells from WT and vavFLIP_R mice were isolated and cultured under T_{H0}, T_{H1}, T_{H2} and T_{H17} polarising conditions, followed by flow cytometry analysis of IFN- γ and IL-17A. (a) Representative dot plots of T_{H1} and T_{H17} differentiated cells are shown. (b) Data are represented as the mean \pm S.E.M. from two independent experiments ($n = 5$ for WT and vavFLIP_R cells). Statistical analyses were performed with two-tailed nonparametric Mann–Whitney *U*-tests. (c) Quantitative real-time PCR analysis of IL-4 mRNA expression in TH2 differentiated WT and vavFLIP_R T cells. Data are represented as the mean \pm S.E.M. from two independent experiments ($n = 4$ for WT and $n = 5$ for vavFLIP_R). (d) EAE was induced by injecting WT and vavFLIP_R mice ($n = 11$) with the MOG₃₅₋₅₅-peptide and two further injections of pertussis toxin. Subsequently, the clinical score was monitored for 40 days. Data are pooled from two independent experiments and represented as the mean \pm S.E.M. (e) WT and vavFLIP_R animals were injected with the MOG₃₅₋₅₅-peptide in complete Freund’s adjuvant. pLN cells isolated 11 (WT $n = 4$, vavFLIP_R $n = 4$) and 14 (WT $n = 5$, vavFLIP_R $n = 3$) days after injection were restimulated with the indicated concentrations of MOG peptide for 24 h, followed by flow cytometry analysis of IFN- γ , IL-17A and IL-4-producing T cells

autoantibodies were identified in sera from vavFLIP_R mice compared with WT mice (Figure 7c).

Multiple organs can be affected in systemic autoimmune diseases. We therefore examined several organs from 1-year-old WT and vavFLIP_R animals by histology. No differences between WT and vavFLIP_R mice could be observed in brains, spleens and pancreas stained with haematoxylin and eosin (H&E) and in spleens stained for B cells and macrophages (data not shown). Kidneys from aged

mice were stained with periodic acid–schiff (PAS) followed by histological scoring. The majority of glomeruli in kidneys from WT mice were normal (Figure 7d). In contrast, thickening of the Bowman’s capsule and protein deposition in glomeruli were observed in kidneys from vavFLIP_R mice, indicating nephropathy (Figure 7e). Glomerular deposition of PAS-positive material is common in aging mice.³⁹ However, significantly more tissue damage was detected in vavFLIP_R kidneys with 63.6% of the kidney sections displaying a

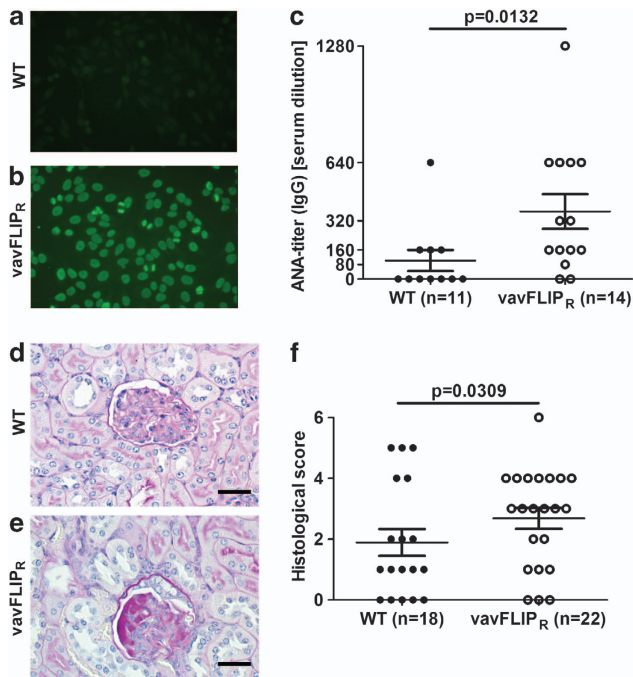


Figure 7 Autoantibody production and nephropathy in aged vavFLIP_R mice. (a–c) Quantification of ANAs in sera from 1-year-old WT ($n = 11$) and vavFLIP_R ($n = 14$) littermates. Representative examples of (a) negative fluorescent pattern (WT) and (b) homogenous ANA pattern (vavFLIP_R). The ANA-IgG titre is shown in (c). Symbols represent individual mice. Horizontal lines represent the mean; error bars display S.E.M. Statistical analysis was performed with two-tailed nonparametric Mann–Whitney *U*-test. (d–f) Kidneys from 1-year-old WT ($n = 18$) and vavFLIP_R ($n = 22$) animals were analysed by histology. (d and e) Representative histological sections of paraffin-embedded kidneys stained with PAS are shown for (d) WT glomerulus with mild thickening of the Bowman’s capsule and (e) vavFLIP_R glomerulus with moderate thickening of the Bowman’s capsule and moderate glomerular protein deposition. Scale bar represents 25 μm . (f) Histological score of PAS-stained kidneys. Individual mice are displayed as separate symbols. Horizontal lines represent the mean; error bars show S.E.M. Animals were divided up into groups of normal alterations (histological score < 3) and moderate-to-severe alterations (histological score 3 or higher), followed by statistical analysis with Fisher’s exact test

histological score of three or higher, implying mild-to-moderate alterations (Figure 7f). In comparison, only 27.8% of kidneys from WT mice manifested similar damage (Figure 7f). Thus, vavFLIP_R mice have a greater degree of nephropathy compared with WT animals at 12–14 months of age.

The histological analyses of lungs from aged mice revealed that three of six vavFLIP_R lungs stained with H&E displayed marked focal interstitial pneumonia compared with one of five WT lungs. Increase in bronchial-associated lymphoid tissue (BALT) has been described in aging mice.⁴⁰ Nevertheless, the amount of BALT was massively increased in four of six vavFLIP_R animals (67%) in comparison with two of five WT mice (40%). Although the composition of BALT was not obviously altered, we detected more IgG-containing immune complexes (Figure 8). Infiltrating macrophages were observed in regions of interstitial pneumonia by immunohistochemical staining for B cells (B220), T cells (CD3) and macrophages (MAC2) in vavFLIP_R lungs (Figure 8). Of note, interstitial pneumonia has occasionally been described for SLE.⁴¹

Taken together, the elevated levels of ANAs and tissue damage in kidneys and lungs are symptoms similar to human SLE.^{41,42} Hence, the kidney damage may be related to the ANAs and represent a mild form of SLE nephropathy.

Discussion

CD95-mediated apoptosis has a crucial role in controlling immune responses and preventing autoimmune diseases.¹ c-FLIP proteins protect cells against CD95-induced apoptosis at the level of the DISC.² Although the isoforms c-FLIP_L and c-FLIP_S have been thoroughly characterised, not much is known about the functional role of c-FLIP_R in the immune system. In this study, we report that constitutive expression of murine c-FLIP_R results in altered lymphocyte populations and lupus-like symptoms with age.

Lpr and *gld* mice with mutations in the CD95 receptor and ligand, respectively, develop lymphoproliferative disease and autoimmunity with accumulation of unusual DN B220⁺ T cells.^{7,29,30,43} c-FLIP proteins inhibit the same apoptosis pathway by preventing caspase-8 cleavage at the DISC.^{15,16} Indeed, T-cell-specific c-FLIP_L transgenic mice were reported to develop autoimmunity when bred on Balb/c, but not C57BL/6, background.²⁵ However, neither altered *Lpr* nor accumulation of DN B220⁺ T cells was identified in up to 1-year-old vavFLIP_R mice, consistent with transgenic mice with T-cell-specific expression of murine c-FLIP_L or human c-FLIP_S in the C57BL/6 background.^{26,27,31} Hence, neither constitutive expression nor overexpression of c-FLIP proteins, at least in the C57BL/6 background, is sufficient for recapitulation of the *lpr/gld* phenotype.

The autoimmune inflammation in EAE is mainly caused by autoreactive T_H1 and T_H17 effector cells.³⁷ *Lpr* mice showed a prolonged and enhanced inflammation in the central nervous system (CNS) upon EAE induction.⁴⁴ Hence, CD95/CD95L interactions are of importance to delete disease-initiating, autoreactive T cells in the CNS in the course of EAE. Both long and short c-FLIP isoforms have been reported to be upregulated in activated T cells from the cerebral spinal fluid in patients with active MS.^{45,46} Interestingly, transgenic mice overexpressing human c-FLIP_L were protected against EAE because of enhanced T_H2 effector responses and consequently reduced T_H1 effector responses.³⁸ Transgenic expression of murine c-FLIP_R did not alter the cytokine production of T cells in a similar way, which may be one reason why the enforced expression of c-FLIP_R only had a minor effect on the progression of EAE. Yu *et al.*⁴⁷ reported high expression levels of c-FLIP_L in T_H17 cells, which protected these cells against AICD. This was proposed to be a mechanism for the high pathogenicity of T_H17 cells in autoimmune diseases. Expression levels of c-FLIP_R in T_H17 cells was not investigated in this study, nevertheless, the increased expression of c-FLIP_L in this cell population may override the effect of the constitutive c-FLIP_R expression in vavFLIP_R mice in the course of EAE. However, the impaired ability of naive vavFLIP_R T cells to differentiate into the T_H17 subset *in vitro* and the minor reduction of effector T-cell responses observed in MOG-immunised vavFLIP_R mice could possibly explain the slightly slower disease progression in vavFLIP_R mice compared with WT littermates.

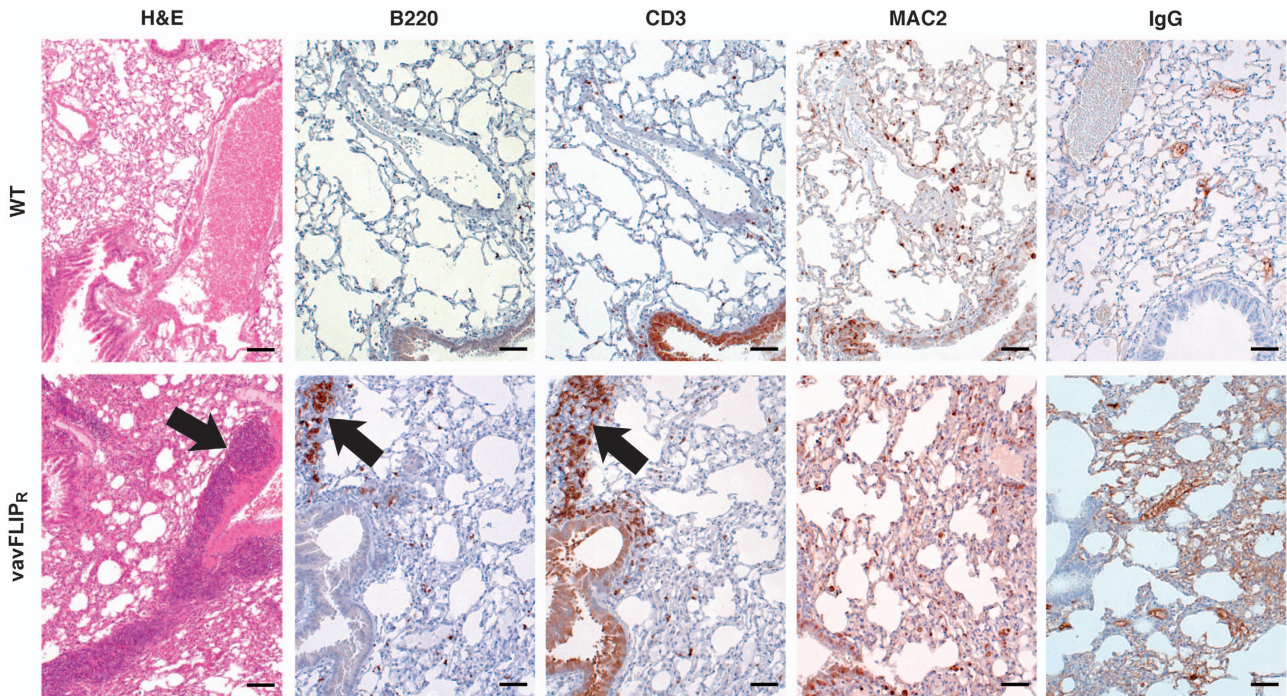


Figure 8 Histological alterations in lungs of aged vavFLIP_R mice. Lungs were prepared from 1-year-old WT ($n = 5$) and vavFLIP_R ($n = 6$) mice and paraffin embedded. Sections were stained with H&E, the B-cell marker B220, the T-cell marker CD3 and the macrophage marker MAC2, respectively. Deposition of IgG-containing immune complexes was detected with goat-anti-mouse antibodies. Representative tissue sections are shown. Arrows indicate increased BALT and interstitial pneumonia, respectively. Scale bars represent 200 μm for H&E section and 50 μm for all other sections

B- and T-cell numbers and distribution were normal in young vavFLIP_R mice²⁸ and no differences in DCs, macrophages, granulocytes or NK cells could be identified even in mice at 1 year of age. Interestingly, aged vavFLIP_R mice had altered lymphocyte populations with lower levels of T cells and higher frequencies of B cells compared with WT littermates. Moreover, reduced levels of CD8⁺ cells were observed, which is consistent with a report of Wu *et al.*⁴⁸ where reduced peripheral CD8⁺ cell numbers were described in mice with transgenic expression of the viral FLIP MC159 under control of the CD2 enhancer cassette. Furthermore, alterations in the ratio of antigen experienced to naive T cells were identified, most probably because of defective AICD. Human c-FLIP_S is upregulated in the activation and expansion phase of an immune response, but is thereafter downregulated to enable AICD and elimination of effector T cells.⁴⁹ We previously described a similar kinetic for murine c-FLIP_R, which explains the defect in AICD upon constitutive c-FLIP_R expression.²⁸ In this study, increased frequencies of activated T helper cells and antigen-experienced T cells as well as lower frequencies and numbers of naive T cells in vavFLIP_R mice compared with WT mice were observed. This is consistent with a previous report where an increased memory T-cell pool was identified in c-FLIP_S transgenic mice compared with WT animals after immunisation with the superantigen staphylococcal enterotoxin B.²⁷ Similarly to the activated T-cell phenotype, vavFLIP_R B cells expressed activation markers to a higher extent than WT B cells. Strikingly, histological analyses of kidneys and lungs from 12 to 14 months old mice revealed a higher degree of nephropathy in vavFLIP_R mice and a larger

proportion of vavFLIP_R animals displayed focal interstitial pneumonia and an increased amount of BALT compared with WT littermates. Moreover, elevated levels of anti-nuclear autoantibodies were identified in vavFLIP_R sera, indicating that vavFLIP_R mice develop a lupus-like phenotype with age. Hence, our findings imply that the altered lymphocyte populations with activated phenotypes in aged vavFLIP_R mice are of functional relevance. Most probably the autoimmune disease observed in vavFLIP_R animals is caused by a combination of autoreactive B and T cells, with persisting CD4⁺ helper T cells, which may prime B cells to produce autoantibodies, and increased levels of B cells. In support of this notion, lupus-like disease was described in c-FLIP_L transgenic mice on the Balb/c background and the development of autoimmunity in this study was shown to require CD4⁺ T cells, which were proposed to result from impaired thymic selection.²⁵ Notably, elevated gene expression of *CFLAR* in CD33⁺ myeloid cells, CD4⁺ T cells and CD19⁺ B cells was reported in SLE patients.⁵⁰ Furthermore, Xu *et al.*⁵¹ observed that human lupus T cells did not downregulate c-FLIP_S after initial activation, which suggests that c-FLIP proteins are of importance in the development of SLE disease. The higher level of T_{reg} cells in aged vavFLIP_R mice is presumably a compensatory mechanism because of the observed autoimmunity. Imbalance of T_{reg} cells has been described in various autoimmune diseases.⁵² Reduced levels or conflicting data have been reported in patients with, for example, juvenile idiopathic arthritis, autoimmune liver disease and myasthenia gravis.⁵² Consistent with our findings, increased levels of T_{reg} cells were identified in patients with

primary Sjögren's syndrome⁵³ and in experimental arthritis in mice.⁵⁴ The expanded T_{reg} cell population observed in 1-year-old vavFLIP_R animals most probably dampens the severity of the SLE-like phenotype.

We previously reported that vavFLIP_R mice are better protected against *Listeria monocytogenes* infection compared with WT littermates.²⁸ Hence, c-FLIP_R expression is beneficial in an acute infection, whereas we in this study demonstrate that chronic expression results in autoimmunity. To conclude, aged vavFLIP_R mice have altered lymphocyte populations with increased levels of antigen-experienced T cells and higher activation status of both B and T cells. Moreover, these animals develop lupus-like symptoms with age. Our results show that c-FLIP_R has an important role in the control of autoimmunity.

Materials and Methods

Mice. vavFLIP_R mice were previously described.²⁸ WT littermates were used as control animals. All animals were kept in a specific pathogen-free environment in the animal facility of Helmholtz Centre for Infection Research, Braunschweig.⁵⁵ C57BL/6 mice were purchased from Harlan Laboratories (Indianapolis, IN, USA) and Charles River (Wilmington, MA, USA). MRL/lpr mice were a kind gift from Dr Detlef Neumann, Hannover Medical School, Hannover, Germany. All breeding and experiments were performed in accordance with the guidelines of national and local authorities.

Cell preparation. Lymphoid organs (pLNs, mesenteric lymph nodes, spleen and thymus) were isolated from mice killed via CO₂. Organs were homogenised through a 70 µm nylon mesh and washed with PBS. Erythrocytes were removed by 2-min incubation in ACK lysis buffer (0.15 M NH₄Cl, 1 mM KHCO₃, 0.1 mM EDTA, pH adjusted to 7.3 with NaOH) at room temperature followed by a further washing step. Primary murine cells were cultured in RPMI 1640 (Gibco – Life technologies, Grand Island, NY, USA) supplemented with 10% FCS (PAA, Pasching, Austria), 50 µg/ml of penicillin and streptomycin (Gibco – Life technologies), 1% non-essential amino acids (Gibco – Life technologies), 2 mM L-glutamine (Gibco – Life technologies) and 1 mM sodium pyruvate (Gibco – Life technologies).

In vitro generation of T helper cell subsets. For differentiation of T helper subsets, CD4⁺CD62L^{high}CD25⁻ naive T cells were sorted by using a FACS Aria II (BD Biosciences, Heidelberg, Germany) or MoFlo (Beckman and Coulter, Indianapolis, IN, USA). Cells were seeded directly after sorting with 2 × 10⁵ cells per well in 96-well plates and activated with plate-bound anti-CD3 and anti-CD28 in the presence of priming cytokines and inhibitory antibodies according to the respective T helper subset: T_H0: 2 µg/ml anti-CD3 (145-2C11, BioLegend, San Diego, CA, USA), 2 µg/ml anti-CD28 (37.51, BioLegend), 10 µg/ml anti-IL-4 (11B11, self-purified) and 10 µg/ml anti-IFN-γ (XMG1.2, self-purified); T_H1: 2 µg/ml anti-CD3 (145-2C11, BioLegend), 2 µg/ml anti-CD28 (37.51, BioLegend), 10 µg/ml anti-IL-4 (11B11, self-purified) and 10 ng/ml IL-12 (R&D Systems, Minneapolis, MN, USA); T_H17: 3 µg/ml anti-CD3 (145-2C11, BioLegend), 5 µg/ml anti-CD28 (37.51, BioLegend), 10 µg/ml anti-IL-2 (JES6-1A12, BioLegend), 10 µg/ml anti-IFN-γ (XMG1.2, self-purified), 2 ng/ml pTGF-β (R&D Systems), 30 ng/ml IL-6 (R&D Systems), 10 ng/ml IL-1-β (R&D Systems) and 20 ng/ml TNF-α (Preprotech, Rocky Hill, NJ, USA). T_H2 cells were differentiated as follows: CD4⁺CD62L^{high}CD25⁻ naive T cells were sorted as above. In all, 2 × 10⁶ cells were seeded after sorting in 24-well plates and activated with plate-bound 5 µg/ml anti-CD3 (145-2C11, BioLegend) and 2 µg/ml anti-CD28 (37.51, BioLegend). After 3 days, 2 × 10⁵ cells were transferred to 96-well plate in the presence of the following priming cytokines and inhibitory antibodies and cultured for additional 3 days: 10 ng/ml murine IL-2 (402-ML, R&D Systems), 10 ng/ml IL-4 (11B11, self-purified), 5 µg/ml anti-IFN-γ (XMG1.2, self-purified) and 5 µg/ml anti-IL12p40 (C17.8, R&D Systems). Subsequently, the differentiated cells were stained for CD4 and either IFN-γ, IL-4 or IL-17A (see staining procedure in the next paragraph) followed by flow cytometry analysis after 4 days of differentiation.

Flow cytometry. Cells were stained with Live/Dead near IR or blue fluorescent reactive dyes (Life Technologies) by incubation for 30 min in

PBS at 4 °C. Thereafter, cells were washed and Fcγ III/II receptors were blocked by incubation with anti-CD16/CD32 (2.4G2, BD Biosciences). Subsequently, cells were washed and stained with antibodies in PBS containing 2% BSA for 20 min at 4 °C. The following antibodies were used: CD3-HorizonV450 (17A2), CD3-FITC (145-2C11), CD4-HorizonV500 (RM4-5), CD8-FITC (53-6.7), CD19-FITC (1D3), CD25-PE Cy7 (PC61.5) (all from BD Biosciences); CD4-Pacific Blue (RM4-5), CD8-APC (53-6.7), CD86-APC (GL-1), I-A/I-E-Alexa Fluor 700 (M5/114.15.2) (all from BioLegend); CD11c-APC eFluor780 (N418), CD19-PerCP Cy5.5 (1D3), CD44-PE (IM7), CD45R (B220)-APC (RA3-6B2), CD49b-APC (Dx5), CD62L-PerCP Cy5.5 (MEL-14), CD69-PE Cy7 (H1.2F3), F4/80-PE (BM8) and Gr1-Pacific Blue (RB6-8C5) (all from eBiosciences, San Diego, CA, USA). Samples were analysed by LSRII or LSRIIFortessa flow cytometers (BD Biosciences). The FlowJo software (TreeStar, Ashland, OR, USA) was used to analyse the data.

Intracellular proteins were stained after surface marker staining. For staining of Foxp3-Alexa Fluor 488, cells were fixed and permeabilised for intracellular cytokine staining by using the Foxp3 Staining Buffer Set (Miltenyi Biotec, Auburn, CA, USA) according to the manufacturer's protocol. For intracellular cytokine staining of IFN-γ-FITC (XMG1.2, BioLegend), IL-4-PE (11B11, eBioscience) and IL-17A-APC (eBio17B7, eBioscience), cells were stimulated for 4 h with PMA and ionomycin (Sigma Aldrich, Munich, Germany), with addition of Brefeldin A (Sigma Aldrich) for the last 2 h, before the staining was performed as for Foxp3.

Real-time detection PCR. cDNA was used as a template for real-time PCR using SYBR Green (Roche, Mannheim, Germany). Ubiquitin C (UBC) was used as reference gene for normalisation. Measurements were performed in duplicates in the LightCycler 96 system (Roche) using the following primers: UBC fwd 5'-AAGAGAATCCACAAGGAATTGAATG-3'; UBC rev 5'-CAACAGGACCTGCTGACAAC-3'; IL4 fwd 5'-CATCGGCATTTTGAACGAG-3'; IL4 rev 5'-CGAGCTCACTCTCTGTGGT-3'.

Experimental autoimmune encephalomyelitis. EAE was induced in 10–12 weeks old WT and vavFLIP_R mice by injecting 200 µg MOG₃₅₋₅₅-peptide (MEVGWYRSPFSRVVHLYRNGK) together with 4 mg/ml mycobacteria in complete Freund's adjuvant subcutaneously at four sites. In all, 200 ng pertussis toxin was injected intraperitoneally to open the blood–brain-barrier. The pertussis toxin injection was repeated 2 days later. Mice were monitored daily for clinical signs of EAE from days 3 to 40 with 0 – no symptoms, 0.5 – partial limp tail, 1 – limp tail, 2 – delayed rotation from dorsal position, 2.5 – hindleg weakness, 3 – complete hindleg paralysis, 3.5 – starting foreleg weakness, 4 – paralysis of one foreleg, 5 – moribund, death. Mice with a score higher than 3 were killed.

For analysis of cytokine-producing T cells, mice were immunised with MOG₃₅₋₅₅-peptide as above, but without pertussis toxin to prevent the migration of primed T cells into the brain. pLNs were isolated from mice killed 11 and 14 days after injection. In all, 5 × 10⁵ cells were seeded per well in 96-well plates and either left untreated or restimulated with plate-bound anti-CD3 (2 µg/ml; 145-2C11, BioLegend) and anti-CD28 (2 µg/ml; 37.51, BioLegend) or up to 50 µg/ml MOG₃₅₋₅₅-peptide for 24 h with addition of 10 µg/ml Brefeldin A (Sigma Aldrich) for the last 2 h. IFN-γ-, IL-4- and IL-17A-producing T cells were analysed by flow cytometry.

Analysis of ANAs. ANAs in sera from 1-year-old WT and vavFLIP_R mice were analysed semiquantitatively by incubating HEp-2 cells seeded on microscope slides (Generic Assays, Dahlewitz, Germany) with sera diluted 1:80–1:1280 for 30 min at room temperature. Slides were washed two times 5 min in PBS followed by incubation with FITC-conjugated donkey anti-mouse IgG (Dianova, Hamburg, Germany) for 30 min in the dark. Thereafter, slides were washed two times 5 min in PBS, transferred to cover slips and sealed. Slides were analysed by fluorescence microscopy where a homogenous pattern was considered as positive for ANAs.

Histology. Kidneys, lungs, livers, spleens, pancreas and brains were isolated from 1-year-old WT and vavFLIP_R mice. Organs were fixed in 4% neutrally buffered formaldehyde and embedded in paraffin for histological analysis. In all, 3 µm sections from organs were stained with H&E. The degree of focal interstitial pneumonia and BALT was determined in H&E-stained lung sections. Lungs were immunohistochemically stained with B220 (RA3-6B2; BD Biosciences), CD3 (SP7; Neo Markers, Fremont, CA, USA) and MAC2 (M3/38; CEDARLANE, Burlington, ON, Canada) to determine lymphocyte and macrophage infiltration. IgG complexes in lung sections were stained with goat-anti-mouse (TM-060-BN, Thermo Fisher Scientific, Waltham, MA, USA). Kidney sections were stained with PAS staining and the sections were analysed for thickening of the Bowman's capsule and

protein casts in glomeruli. Scoring was performed in a blinded manner for each criterion as follows: 0 – no alteration, 1 – low grade (slightly visible), 2 – moderate (clearly visible), 3 – severe (dominant finding). Scores were added to a total score for each organ.

Statistical analyses. Statistical analyses were performed by nonparametric Mann–Whitney *U*-test or Fisher's exact test using GraphPad Prism software (Graph Pad Software, La Jolla, CA, USA). Data are presented as the mean with S.E.M. and S.D. as error bars.

Conflict of Interest

The authors declare no conflict of interest.

Acknowledgements. We are grateful to Sabrina Schumann, Dominique Gollasch and Lena Seela for expert technical assistance, Anne-Marie Matthies for help with Ig ELISAs and Dr Marc Schuster for critically reading the manuscript. We thank Dr Detlef Neumann for providing us with MRL/lpr mice and Dr Jochen Huehn for various reagents. Moreover, we appreciate the excellent support from the FACS facility, especially Dr Lothar Groebe, and the animal facility, in particular David Dettbarn, at the Helmholtz Centre for Infection Research. We also thank Dr Frank Klawonn for assistance with statistical analyses. FE, MA and CP-S were supported by the President's Initiative and Networking Fund of the Helmholtz Association of German Research Centers (HGF) under contract number VH-GS-202. This project was funded by the DFG (SCHM1586/2-1 and SCHM1586/2-2).

- Bouillet P, O'Reilly LA. CD95, BIM and T cell homeostasis. *Nat Rev Immunol* 2009; **9**: 514–519.
- Krammer PH, Arnold R, Lavrik IN. Life and death in peripheral T cells. *Nat Rev Immunol* 2007; **7**: 532–542.
- Alderson MR, Tough TW, Davis-Smith T, Braddy S, Falk B, Schooley KA *et al*. Fas ligand mediates activation-induced cell death in human T lymphocytes. *J Exp Med* 1995; **181**: 71–77.
- Dhein J, Walczak H, Baumler C, Debatin KM, Krammer PH. Autocrine T-cell suicide mediated by APO-1/(Fas/CD95). *Nature* 1995; **373**: 438–441.
- Brunner T, Mogil RJ, LaFace D, Yoo NJ, Mahboubi A, Echeverri F *et al*. Cell-autonomous Fas (CD95)/Fas-ligand interaction mediates activation-induced apoptosis in T-cell hybridomas. *Nature* 1995; **373**: 441–444.
- Ju ST, Panka DJ, Cui H, Ettinger R, el-Khatib M, Sherr DH *et al*. Fas(CD95)/FasL interactions required for programmed cell death after T-cell activation. *Nature* 1995; **373**: 444–448.
- Cohen PL, Eisenberg RA. Lpr and gld: single gene models of systemic autoimmunity and lymphoproliferative disease. *Annu Rev Immunol* 1991; **9**: 243–269.
- Sneller MC, Straus SE, Jaffe ES, Jaffe JS, Fleisher TA, Stetler-Stevenson M *et al*. A novel lymphoproliferative/autoimmune syndrome resembling murine lpr/gld disease. *J Clin Invest* 1992; **90**: 334–341.
- Peter ME, Krammer PH. The CD95(APO-1/Fas) DISC and beyond. *Cell Death Differ* 2003; **10**: 26–35.
- Kischkel FC, Hellbardt S, Behrmann I, Germer M, Pawlita M, Krammer PH *et al*. Cytotoxicity-dependent APO-1 (Fas/CD95)-associated proteins form a death-inducing signaling complex (DISC) with the receptor. *EMBO J* 1995; **14**: 5579–5588.
- Boatright KM, Rensatus M, Scott FL, Sperandio S, Shin H, Pedersen IM *et al*. A unified model for apical caspase activation. *Mol Cell* 2003; **11**: 529–541.
- Donepudi M, Mac Sweeney A, Briand C, Grutter MG. Insights into the regulatory mechanism for caspase-8 activation. *Mol Cell* 2003; **11**: 543–549.
- Li J, Yuan J. Caspases in apoptosis and beyond. *Oncogene* 2008; **27**: 6194–6206.
- Fischer U, Janicke RU, Schulze-Osthoff K. Many cuts to ruin: a comprehensive update of caspase substrates. *Cell Death Differ* 2003; **10**: 76–100.
- Scaffidi C, Schmitz I, Krammer PH, Peter ME. The role of c-FLIP in modulation of CD95-induced apoptosis. *J Biol Chem* 1999; **274**: 1541–1548.
- Krueger A, Schmitz I, Baumann S, Krammer PH, Kirchhoff S. Cellular FLICE-inhibitory protein splice variants inhibit different steps of caspase-8 activation at the CD95 death-inducing signaling complex. *J Biol Chem* 2001; **276**: 20633–20640.
- Golks A, Brenner D, Fritsch C, Krammer PH, c-FLIP_R Lavrik IN. A new regulator of death receptor-induced apoptosis. *J Biol Chem* 2005; **280**: 14507–14513.
- Imler M, Thome M, Hahne M, Schneider P, Hofmann K, Steiner V *et al*. Inhibition of death receptor signals by cellular FLIP. *Nature* 1997; **388**: 190–195.
- Fuentes-Prior P, Salvesen GS. The protein structures that shape caspase activity, specificity, activation and inhibition. *Biochem J* 2004; **384**(Pt 2): 201–232.
- Jeuffing N, Singh KK, Christians A, Thorns C, Feller AC, Nagl F *et al*. A single nucleotide polymorphism determines protein isoform production of the human c-FLIP protein. *Blood* 2009; **114**: 572–579.
- Jeuffing N, Keil E, Freund C, Kuhne R, Schulze-Osthoff K, Schmitz I. Mutational analyses of c-FLIP_R, the only murine short FLIP isoform, reveal requirements for DISC recruitment. *Cell Death Differ* 2008; **15**: 773–782.
- Fricker N, Beaudouin J, Richter P, Eils R, Krammer PH, Lavrik IN. Model-based dissection of CD95 signaling dynamics reveals both a pro- and antiapoptotic role of c-FLIP_L. *J Cell Biol* 2010; **190**: 377–389.
- Micheau O, Thome M, Schneider P, Holler N, Tschopp J, Nicholson DW *et al*. The long form of FLIP is an activator of caspase-8 at the Fas death-inducing signaling complex. *J Biol Chem* 2002; **277**: 45162–45171.
- Chang DW, Xing Z, Pan Y, Algeciras-Schminich A, Barnhart BC, Yaish-Ohad S *et al*. c-FLIP(L) is a dual function regulator for caspase-8 activation and CD95-mediated apoptosis. *EMBO J* 2002; **21**: 3704–3714.
- Qiao G, Li Z, Minto AW, Shia J, Yang L, Bao L *et al*. Altered thymic selection by overexpressing cellular FLICE inhibitory protein in T cells causes lupus-like syndrome in a BALB/c but not C57BL/6 strain. *Cell Death Differ* 2010; **17**: 522–533.
- Hinshaw-Makepeace J, Huston G, Fortner KA, Russell JQ, Holoch D, Swain S *et al*. c-FLIP(S) reduces activation of caspase and NF-kappaB pathways and decreases T cell survival. *Eur J Immunol* 2008; **38**: 54–63.
- Oehme I, Neumann F, Bossler S, Zornig M. Transgenic overexpression of the Caspase-8 inhibitor FLIP(short) leads to impaired T cell proliferation and an increased memory T cell pool after staphylococcal enterotoxin B injection. *Eur J Immunol* 2005; **35**: 1240–1249.
- Teliëps T, Ewald F, Gereke M, Annemann M, Rauter Y, Schuster M *et al*. Cellular-FLIP, Raji isoform (c-FLIP_R) modulates cell death induction upon T-cell activation and infection. *Eur J Immunol* 2013; **43**: 1499–1510.
- Watanabe-Fukunaga R, Brannan CI, Copeland NG, Jenkins NA, Nagata S. Lymphoproliferative disorder in mice explained by defects in Fas antigen that mediates apoptosis. *Nature* 1992; **356**: 314–317.
- Yasutomo K, Maeda K, Nagata S, Nagasawa H, Okada K, Good RA *et al*. Defective T cells from gld mice play a pivotal role in development of Thy-1.2 + B220 + cells and autoimmunity. *J Immunol* 1994; **153**: 5855–5864.
- Lens SM, Kataoka T, Fortner KA, Tinel A, Ferrero I, MacDonald RH *et al*. The caspase 8 inhibitor c-FLIP(L) modulates T-cell receptor-induced proliferation but not activation-induced cell death of lymphocytes. *Mol Cell Biol* 2002; **22**: 5419–5433.
- Leverkus M, Walczak H, McLellan A, Fries HW, Terbeck G, Brocker EB *et al*. Maturation of dendritic cells leads to up-regulation of cellular FLICE-inhibitory protein and concomitant down-regulation of death ligand-mediated apoptosis. *Blood* 2000; **96**: 2628–2631.
- Huang QQ, Perlman H, Huang Z, Birkett R, Kan L, Agrawal H *et al*. FLIP: a novel regulator of macrophage differentiation and granulocyte homeostasis. *Blood* 2010; **116**: 4968–4977.
- Sakaguchi S. Regulatory T cells: key controllers of immunologic self-tolerance. *Cell* 2000; **101**: 455–458.
- Hori S, Nomura T, Sakaguchi S. Control of regulatory T cell development by the transcription factor Foxp3. *Science* 2003; **299**: 1057–1061.
- Iglesias A, Bauer J, Litzenburger T, Schubart A, Linington C. T- and B-cell responses to myelin oligodendrocyte glycoprotein in experimental autoimmune encephalomyelitis and multiple sclerosis. *Glia* 2001; **36**: 220–234.
- Fletcher JM, Lalor SJ, Sweeney CM, Tubridy N, Mills KH. T cells in multiple sclerosis and experimental autoimmune encephalomyelitis. *Clin Exp Immunol* 2010; **162**: 1–11.
- Tseveleki V, Bauer J, Taoufik E, Ruan C, Leondiadis L, Haralambous S *et al*. Cellular FLIP (long isoform) overexpression in T cells drives Th2 effector responses and promotes immunoregulation in experimental autoimmune encephalomyelitis. *J Immunol* 2004; **173**: 6619–6626.
- Maronpot RR BG, Gaul BW. *Pathology of the Mouse*. Cache River Press: St Louis, MO, USA, 1999, p 699.
- Pettan-Brewer C, Treuting PM. Practical pathology of aging mice. *Pathobiol Aging Age Related Dis* 2011; **1**: doi:10.3402/pba.v1i0.7202.
- Cheema GS, Quismorio FP Jr. Interstitial lung disease in systemic lupus erythematosus. *Curr Opin Pulm Med* 2000; **6**: 424–429.
- Munoz LE, Gaipil US, Franz S, Sheriff A, Voll RE, Kalden JR *et al*. SLE—a disease of clearance deficiency? *Rheumatology (Oxford)* 2005; **44**: 1101–1107.
- Budd RC, Van Houten N, Clements J, Mixer PF. Parallels in T lymphocyte development between lpr and normal mice. *Semin Immunol* 1994; **6**: 43–48.
- Suvannavejh GC, Dal Canto MC, Matis LA, Miller SD. Fas-mediated apoptosis in clinical remissions of relapsing experimental autoimmune encephalomyelitis. *J Clin Invest* 2000; **105**: 223–231.
- Sharief MK. Increased cellular expression of the caspase inhibitor FLIP in intrathecal lymphocytes from patients with multiple sclerosis. *J Neuroimmunol* 2000; **111**: 203–209.
- Semra YK, Seidi OA, Sharief MK. Overexpression of the apoptosis inhibitor FLIP in T cells correlates with disease activity in multiple sclerosis. *J Neuroimmunol* 2001; **113**: 268–274.
- Yu Y, Iclozan C, Yamazaki T, Yang X, Anasetti C, Dong C *et al*. Abundant c-Fas-associated death domain-like interleukin-1-converting enzyme inhibitory protein expression determines resistance of T helper 17 cells to activation-induced cell death. *Blood* 2009; **114**: 1026–1028.

48. Wu Z, Roberts M, Porter M, Walker F, Wherry EJ, Kelly J *et al*. Viral FLIP impairs survival of activated T cells and generation of CD8⁺ T cell memory. *J Immunol* 2004; **172**: 6313–6323.
49. Kirchhoff S, Muller WW, Li-Weber M, Krammer PH. Up-regulation of c-FLIPshort and reduction of activation-induced cell death in CD28-costimulated human T cells. *Eur J Immunol* 2000; **30**: 2765–2774.
50. Hutcheson J, Scatizzi JC, Siddiqui AM, Haines GK 3rd, Wu T, Li QZ *et al*. Combined deficiency of proapoptotic regulators Bim and Fas results in the early onset of systemic autoimmunity. *Immunity* 2008; **28**: 206–217.
51. Xu L, Zhang L, Yi Y, Kang HK, Datta SK. Human lupus T cells resist inactivation and escape death by upregulating COX-2. *Nat Med* 2004; **10**: 411–415.
52. DeJaco C, Duftner C, Grubeck-Loebenstien B, Schirmer M. Imbalance of regulatory T cells in human autoimmune diseases. *Immunology* 2006; **117**: 289–300.
53. Gottenberg JE, Lavie F, Abbed K, Gasnault J, Le Nevot E, Delfraissy JF *et al*. CD4⁺CD25^{high} regulatory T cells are not impaired in patients with primary Sjogren's syndrome. *J Autoimmun* 2005; **24**: 235–242.
54. Monte K, Wilson C, Shih FF. Increased number and function of FoxP3 regulatory T cells during experimental arthritis. *Arthritis Rheum* 2008; **58**: 3730–3741.
55. Stehr M, Greweling MC, Tischer S, Singh M, Blocker H, Monner DA *et al*. Charles River altered Schaedler flora (CRASF) remained stable for four years in a mouse colony housed in individually ventilated cages. *Lab Anim* 2009; **43**: 362–370.



Cell Death and Disease is an open-access journal published by *Nature Publishing Group*. This work is licensed under a Creative Commons Attribution-NonCommercial-ShareAlike 3.0 Unported License. The images or other third party material in this article are included in the article's Creative Commons license, unless indicated otherwise in the credit line; if the material is not included under the Creative Commons license, users will need to obtain permission from the license holder to reproduce the material. To view a copy of this license, visit <http://creativecommons.org/licenses/by-nc-sa/3.0/>

Supplementary Information accompanies this paper on Cell Death and Disease website (<http://www.nature.com/cddis>)